

# Transient RF Signals During the Switching of MESFET Control Devices

Nitin Jain, Ronald J. Gutmann, *Senior Member, IEEE*, and David M. Johnson

**Abstract**—An analytical model that predicts the intrinsic small-signal switching transients for MESFET control devices is developed. Theoretical results for video-breakthrough and small signal RF switching waveforms are in excellent agreement with measurements on many devices. Although the intrinsic transients are less than a few nanoseconds in duration, FET material aspects (such as surface states) can induce much longer transients. The 10–90% switching time, which is dominated by intrinsic effects, can be lowered by reducing gate length and gate bias resistance (the latter is more feasible with recently reported diode-gate FET's).

## I. INTRODUCTION

GaAs MESFET's are increasingly being used for such broad-band control applications as switches and variable attenuators because the control port (the gate) is isolated from the RF ports (source and drain), the MESFET consumes little prime power in either state, and the device is compatible with conventional MMIC processing. Previous work [1] has examined the steady-state small-signal performance and high-power capabilities of MESFET control devices, while in this paper transient characteristics are examined. The small-signal RF transients can be broadly classified as intrinsic device-related transients or material-related transients.

The intrinsic device-related transients refer to the transient signals that originate as the depletion layer is switched. For conventional control FET's, lower limits to rise and fall times and the video breakthrough (defined as the signal induced in the output port by switching of the control signal) result from intrinsic transients. When the device is switched into the conducting state from the nonconducting state (i.e., switched “on”) the incremental gate capacitance progressively increases during the transient. The bias resistance, which usually is much larger than other resistances, together with the gate–channel capacitance, determines the intrinsic charging time (and, therefore, the RF signal rise time). When the switch goes from the conducting state to the nonconducting state (i.e., switched “off”), these processes are reversed. The video breakthrough results from the depletion layer charge being switched.

Besides these normal transients, abnormally long material-induced transients are important for many applica-

Manuscript received February 27, 1990; revised July 23, 1990. This work was supported by M/A-COM under a grant administered by G. DiPiazza and D. Maki.

N. Jain and R. J. Gutmann are with the Department of Electrical, Computer and System Engineering and the Center for Integrated Electronics, Rensselaer Polytechnic Institute, Troy, NY 12180.

D. M. Johnson is with the Advanced Semiconductor Division, M/A-COM, Lowell, MA 01851.

IEEE Log Number 9040563.

tions of MESFET control devices [2]–[4]. Surface states, deep traps, and defects in the channel and S.I. substrate can play a significant role in the beyond-microsecond switching waveforms. The effect of these states is evident in extended values for the last-1% settling time in the case of switches and extended values for the 10–90% rise times in multibit attenuators, variable attenuators, and phase shifters.

In addition to these issues, which are relevant to conventional MESFET control devices with resistive gate bias circuits, the recently described diode-gate MESFET for base-band applications poses new switching considerations. The Schottky diode in the diode-gate MESFET can dominate the switching transients unless properly designed [5], [6]. There is a trade-off between the diode size and the peak positive bias on the MESFET in the conducting state to allow intrinsic RF switching transients in the nanosecond range [6].

In Section II, analytical models to simulate the intrinsic switching transients are developed. The models can be easily implemented on SPICE and are useful in predicting the rise and fall times and the video breakthrough for conventional control MESFET's. In Section III, the results from this model are compared with experimental results, and various trade-offs are examined. In Section IV we examine the material-induced abnormal transients. A technique to measure the last-1% settling time for a SPST MESFET switch is presented together with measurement results on switches and variable attenuators. In Section V we discuss the important results and indicate possible device improvements.

## II. MODELING OF INTRINSIC TRANSIENTS

The transition between the nonconducting state and the conducting state can be divided into two regions. In region 1, the depletion layer extends into the substrate and the significant intrinsic capacitance is the gate sidewall capacitance, as shown in Fig. 1(a). This incremental capacitance depends upon gate voltage as given by [7]

$$C_{tgds} = \epsilon W \tan^{-1} \sqrt{\frac{V_{bi} - V_p}{V_p - V_{gd,gs}}} \quad (1)$$

where  $V_p$  is the applied voltage at the gate to completely deplete the channel,  $V_{gd}$  and  $V_{gs}$  are the gate-to-drain and gate-to-source voltages respectively (since we are considering small-signal switching, these voltages are equal),  $V_{bi}$  is the built-in bias voltage (positive),  $W$  is the gate width, and  $\epsilon$  is the permittivity of GaAs. In the second region the depletion layer is confined to the channel region, as shown in Fig. 1(b). The sidewall capacitance can be easily obtained using a procedure similar to that of Takada *et al.* [7]. The capaci-

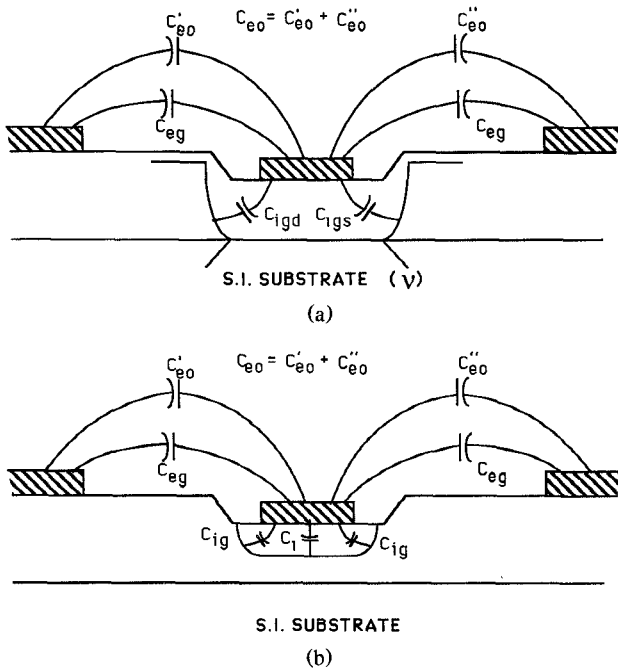


Fig. 1. The relevant capacitances that determine the GaAs MESFET small-signal switching transients. (a) Gate voltage less than pinch-off. (b) Gate voltage more than pinch-off.

tance  $C_{ig}$  is given as

$$C_{ig} = \epsilon W \frac{\pi}{2}. \quad (2)$$

The other important capacitance is the depletion layer capacitance,  $C_i$ , in Fig. 1(b). This depletion layer capacitance is given as

$$C_i = LW \sqrt{\frac{\epsilon q N_d}{2(V_{bi} - V_g)}} \quad (3)$$

where  $L$  is the gate length and  $V_g$  is the gate voltage with respect to the channel (excluding the built-in voltage,  $V_{bi}$ ).

In addition to these intrinsic capacitances, additional extrinsic capacitances are present owing to the gate-to-drain and gate-to-source metal pad couplings and gate-drain overlay in interdigitated devices. These capacitances are layout dependent [1] and are indicated as  $C_{eg}$  and  $C_{eo}$  in Fig. 1.  $C_{eg}$  is the coupling between the gate finger and the source or drain finger, while  $C_{eo}$  represents the total layout-dependent coupling capacitances including the metal overlay capacitances. Since the gate length is typically small (about a micron) and the gate-bias resistance very large (in  $k\Omega$ 's), the distributive effect of the gate-to-channel capacitance-resistance network on the transient RF signal is very small.

With this approximation the gate-to-channel region can be lumped into discrete nonlinear elements viewed from the gate circuit. For most control MESFET's the device resistance is much smaller than the characteristic impedance, and therefore the various capacitances can be combined into a single capacitance in series with  $25 \Omega$  and the gate bias resistance, as is shown in Fig. 2. The capacitance  $C'$  is equal to  $[2(C_{igd} + C_{eg}) + C_{eo}]$  in region 1 of the switching transient and  $[2(C_{ig} + C_{eg}) + C_i + C_{eo}]$  in region 2. The capacitance  $C'$  decreases abruptly when the pinch-off voltage is attained,

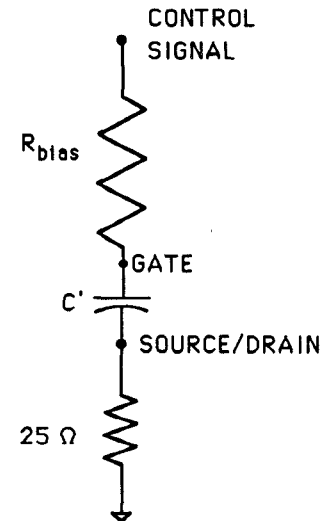


Fig. 2. The simplified equivalent circuit used for analyzing the small-signal intrinsic switching transients.

because the depletion layer capacitance decreases abruptly when the depletion layer meets the S.I. substrate. When the conducting-state MESFET resistance becomes significant compared with the characteristic impedance, additional resistive elements accounting for the conducting state resistance have to be introduced.

When the FET is switched "on" the control voltage changes from  $V_{bias}$  to 0 V. Usually the off-to-on transition is fast enough that generation current does not play any significant role in determining the switching transients. Under this assumption, the following equation for the gate-to-channel voltage is obtained:

$$(R_{bias} + 25)C' \frac{dV_g}{dt} + V_g = \begin{cases} V_{bias} \left(1 - \frac{t}{\tau_u}\right) & t < \tau_u \\ 0 & t \geq \tau_u \end{cases} \quad (4)$$

where the initial condition is  $V_g(t=0) = V_{bias}$ .

Similarly the "on" to "off" transition is represented by the following equation:

$$(R_{bias} + 25)C' \frac{dV_g}{dt} + V_g = \begin{cases} V_{bias} \frac{t}{\tau_d} & t < \tau_d \\ V_{bias} & t \geq \tau_d \end{cases} \quad (5)$$

where the initial condition  $V_g(t=0) = 0$  V.

Though only linear ramp voltages have been analyzed, the right-hand sides of (4) and (5) can have arbitrary time dependence. For such arbitrary switching waveforms these equations can be solved numerically. The gate voltage thus obtained can then be used to calculate the transient RF signal.

When the control pulse can be approximated as a step function, the right sides of (4) and (5) reduce to zero and  $V_{bias}$  for all times, respectively. Equation (4) representing the "on" transition can then be easily integrated to obtain

$$t = (RC_{eo} + 2RC_{eg}) \ln \frac{V_{bias}}{V_g(t)} - \int_{V_{bias}}^{V_g(t)} \frac{2R\epsilon W}{V} \tan^{-1} \sqrt{\frac{V_{bi} - V_p}{V_p - V}} dV \quad \text{for } V_g(t) < V_p \quad (6a)$$

where  $R = (R_{\text{bias}} + 25)$ . Equation (6a) models the transient region where the channel is completely depleted (represented in Fig. 1(a)). Equation (6a) can be used to calculate  $T_1$ , which is defined as the time when the channel has just reached the point of complete depletion, i.e.,

$$T_1 \equiv t(V_p). \quad (6b)$$

For time  $t$  greater than  $T_1$ , the capacitance  $C'$  is given by a different equivalent circuit; therefore, a new equation relating  $t$  and  $V_g(t)$  is obtained for this region of the transient:

$$t = T_1 + R(\epsilon W \pi + 2C_{eg} + C_{eo}) \ln \frac{V_p}{V_g(t)} + LW \sqrt{\frac{\epsilon q N_d}{2V_{bi}}} R \left[ \ln \frac{\sqrt{V_{bi} - V_p} - \sqrt{V_{bi}}}{\sqrt{V_{bi} - V_p} + \sqrt{V_{bi}}} - \ln \frac{\sqrt{V_{bi} - V_g(t)} - \sqrt{V_{bi}}}{\sqrt{V_{bi} - V_g(t)} + \sqrt{V_{bi}}} \right] \quad \text{for } V_g(t) > V_p. \quad (6c)$$

Similarly, the "off" transition is obtained by integrating (5), and the following equation is obtained:

$$t = R(\epsilon W \pi + 2C_{eg} + C_{eo}) \ln \frac{V_{bias}}{V_{bias} - V_{g(t)}} + LW \sqrt{\frac{\epsilon q N_d}{2(V_{bi} - V_{bias})}} \cdot R \left[ \ln \frac{\sqrt{V_{bi} - V_{bias}} + \sqrt{V_{bi} - V_g(t)}}{\sqrt{V_{bi} - V_{bias}} - \sqrt{V_{bi} - V_g(t)}} - \ln \frac{\sqrt{V_{bi} - V_{bias}} + \sqrt{V_{bi}}}{\sqrt{V_{bi} - V_{bias}} - \sqrt{V_{bi}}} \right] \quad \text{for } V_g(t) > V_p \quad (7a)$$

where  $R = R_{\text{bias}} + 25 \Omega$ . Again,  $T_2$  (defined as the time when the channel has just reached the point of complete depletion) can be calculated from (7a), i.e.,

$$T_2 \equiv t(V_p). \quad (7b)$$

For time  $t$  greater than  $T_2$ , the channel is completely depleted and the equation relating  $t$  and  $V_g(t)$  is given as

$$t = T_2 + 2R\epsilon W \int_{V_p}^{V_g(t)} \left[ \frac{1}{V_{bias} - V} \right] \left[ \tan^{-1} \sqrt{\frac{V_{bi} - V_p}{V_p - V}} \right] dV + R(2C_{eg} + C_{eo}) \ln \frac{V_{bias} - V_p}{V_{bias} - V_g(t)} \quad \text{for } V_g(t) < V_p. \quad (7c)$$

The integrals in (6a) and (7c) can be approximated depending on  $V_{bias}$ .

### III. RESULTS OF INTRINSIC TRANSIENTS

Equations (4) and (5) were used to generate the video breakthrough signal by calculating the time-dependent voltage at the gate and then using circuit equations to generate the output waveform. Fig. 3 shows the video breakthrough signal for a single series mounted control MESFET when the control pulse rise time is about 0.5 nS. The figure shows that the actual experimental results are in excellent agreement

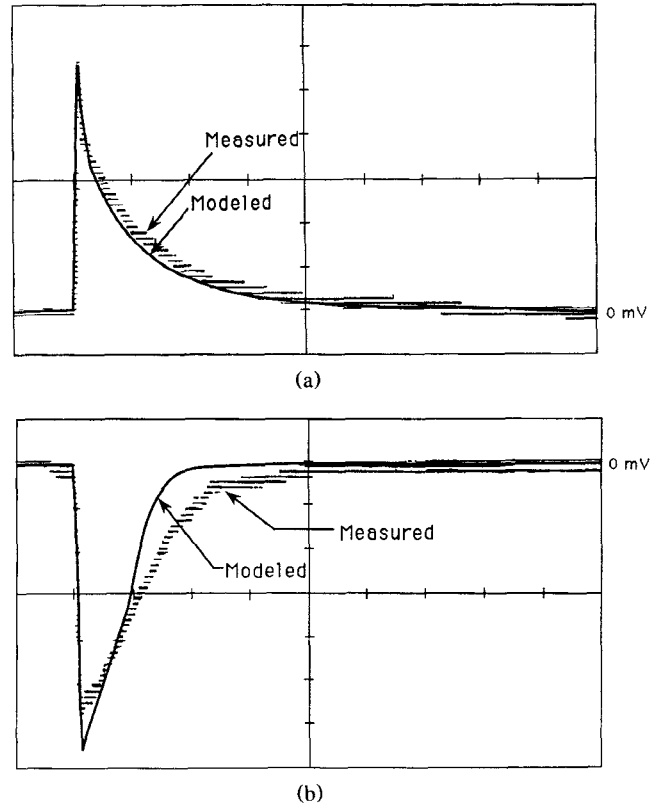


Fig. 3. The measured and modeled video-breakthrough signals for a series mounted control MESFET (with pinch-off of  $-3.5$  V). (a) Bias voltage switched for  $-7$  to  $0$  V. (b) Bias voltage switched from  $0$  to  $-7$  V. The horizontal scale is  $5$  ns/div and the vertical scale  $5$  mV/div.

with the theoretical results. The transition from the off state to on state has a long tail because the flat-wall capacitance increases as the gate bias is increased, and therefore the rate of gate voltage increase with time successively decreases. In the "on" to "off" transition the depletion layer width is increasing, thereby decreasing the incremental capacitance. As a result, the rate of voltage increase with time successively increases.

The complete RF response of a control component due to the control generator pulse was simulated using SPICE. The capacitances were approximated by polynomial fits while the standard MESFET device model was fitted to give the appropriate resistance in the linear region of the curve. The capacitance  $C_i$  changes abruptly at  $V_p$ ; therefore no polynomial fit for this capacitance is appropriate. However, it is sufficient to have a good fit only below pinch-off, because beyond pinch-off the channel resistance rises rapidly and the exact value of  $C_i$  is immaterial (as it does not affect the sidewall capacitance charging time).

The RF switching waveform of the modified dual 2-throw control component described previously was studied [1]. The experimental results of the RF response are given in Fig. 4, along with the results of the SPICE simulation. The initial dc offset in the RF signal can be understood in terms of the video breakthrough being superimposed on the RF signal. Notice that during the "off" to "on" transition the shift that is observed is positive, as expected, while in the "on" to "off" transition the RF waveform is lowered (again as expected).

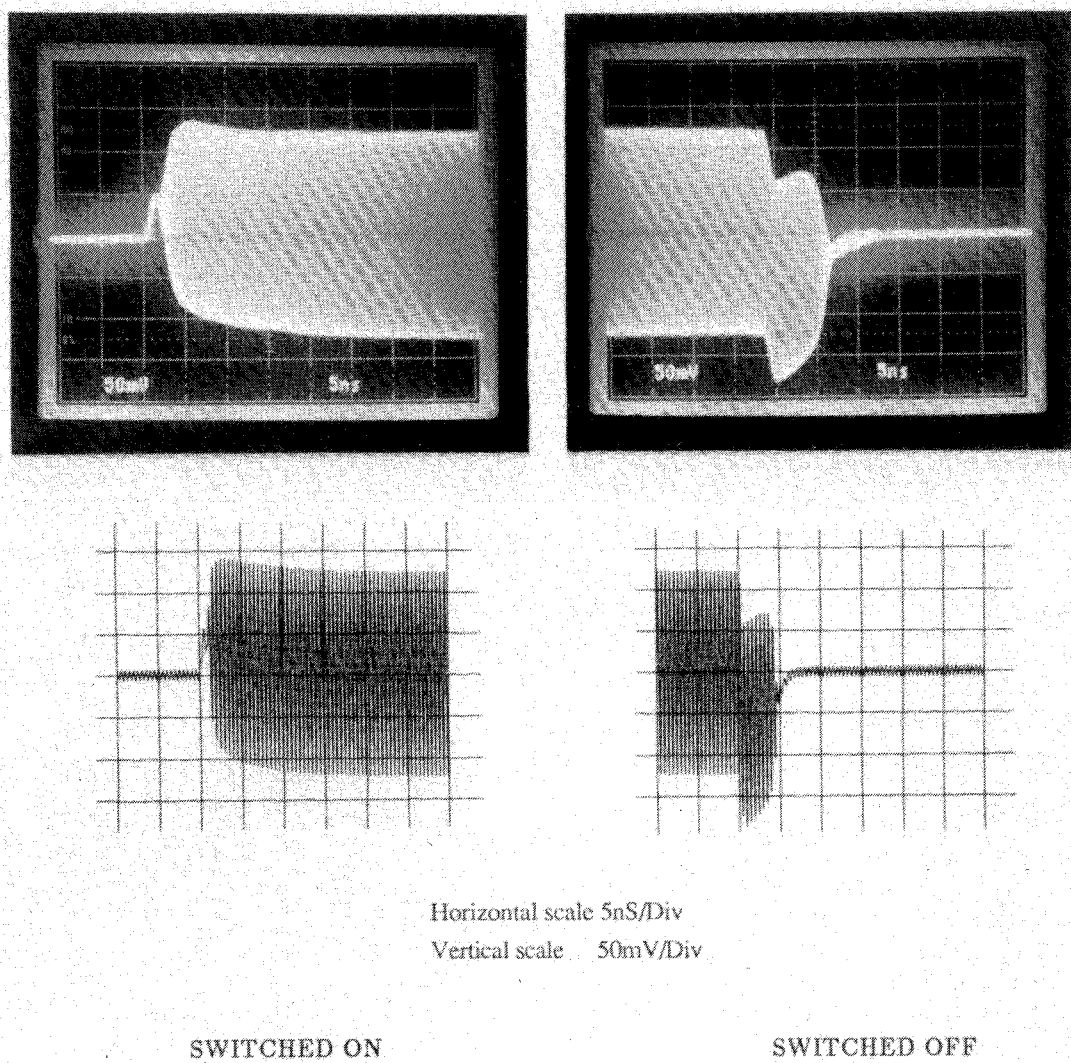


Fig. 4. The measured and simulated RF switching transient for a modified dual-2 throw [1] control component when the device is being switched on and off. Bias voltages are 0 and  $-7$  V.

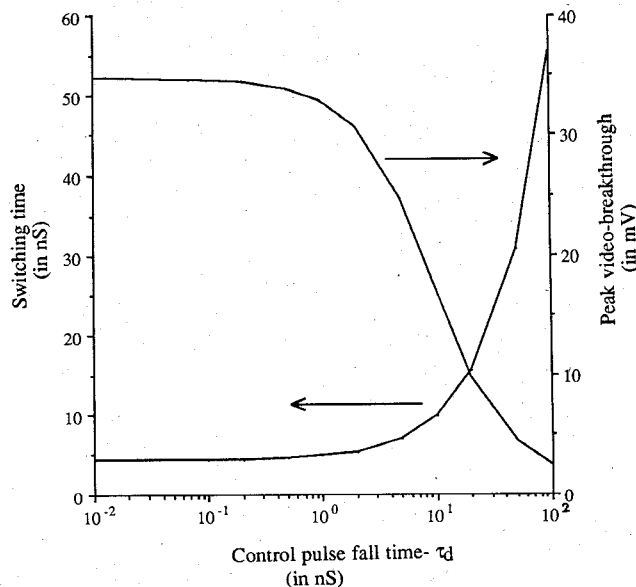


Fig. 5. The trade-off between the switching speed and the peak video breakthrough for a discrete series mounted control MESFET.

An analysis was carried out using (4) and (5) to calculate the peak video breakthrough and RF fall times (defined here as the time in which the RF signal falls by 90%) during the off transition when the fall time for the control pulses was varied. Fig. 5 plots the RF fall time and peak video breakthrough signal with various control pulse fall times. The graph shows that the peak video breakthrough signal can be traded with fall time to a certain extent. Similar results were also seen for the on transition. With control voltage transients below 1 nS, (6) and (7) can also be used to analyze the switching transient.

#### IV. MATERIAL-INDUCED TRANSIENTS

Material-induced "off" to "on" transients are difficult to measure for a discrete control MESFET because a typical control MESFET in a  $50\ \Omega$  environment has a very low impedance (about  $2-3\ \Omega$ ) in the conducting state. Any small variation in the effective impedance of the MESFET has little effect on the output. When a number of these MESFET's are cascaded the transient effects are enhanced, resulting in extraordinarily long rise times. For example, rise

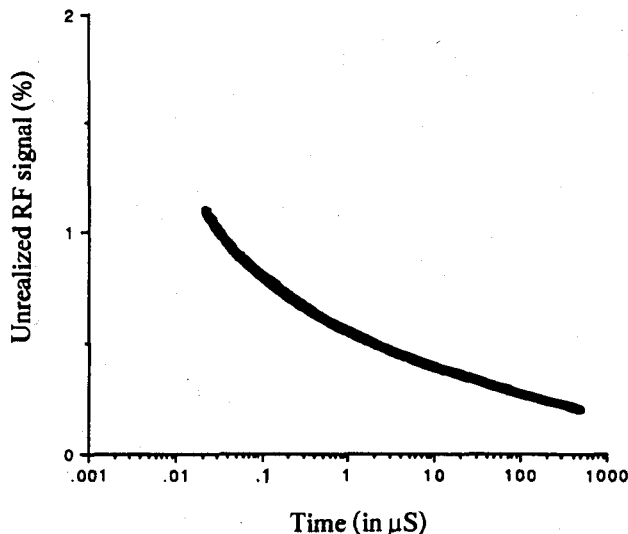


Fig. 6. The unrealized RF signal with time for a 1.2 mm MESFET control device. The data points represent scaled values from measurement of 75  $\mu\text{m}$  MESFET devices.

times more than 1  $\mu\text{s}$  are not abnormal for 32 control FET's in cascade. It is important to quantify and understand this behavior.

As mentioned earlier, the material-induced transients are extremely difficult to measure on a single control FET because the output RF waveform is only slightly modulated. To measure the material-induced transients we used 75  $\mu\text{m}$  (gate width) FET's instead of the 1.2 mm FET's typically used for circuit applications. These FET's have a much higher conducting-state impedance and, therefore, any channel impedance modulation would be quite large in a 50  $\Omega$  environment. A small-signal RF waveform was introduced at the drain, and the RF waveform at the source was monitored as the gate was switched. The magnitude of the waveform was recorded at different times and the result scaled to a 1.2 mm device by dividing the measured resistance by the ratio of the gate periphery. Fig. 6 shows the time dependence of the unrealized signal (i.e., the difference between the steady-state RF level and the time-dependent transient value expressed as a percentage). Since in the first few tens of nanoseconds the intrinsic transient signal is present, the measured values have an additional transient in this region.

Besides measuring the last-1% settling times of a control MESFET, we also measured the 10–90% rise time of a variable attenuator. The variable attenuator contained a single FET having a nominal pinch-off voltage of -3.5 V that was successively switched from -7 V to a bias voltage between 0 and the pinch-off voltage. Fig. 7 shows the 10–90% rise time with various attenuation settings, where it is seen that the RF waveform at higher attenuation settings has higher 10–90% rise times.

These abnormal rise times can be explained qualitatively in terms of surface states (which play the dominant role for these transition) [3], deep traps in the channel, and S.I. substrate related traps and defects. It is well known that the GaAs surface is difficult to passivate and has substantial surface states. When the gate is biased negatively, electrons can easily transit into available surface states. The surface becomes more negative with respect to the bulk, thereby

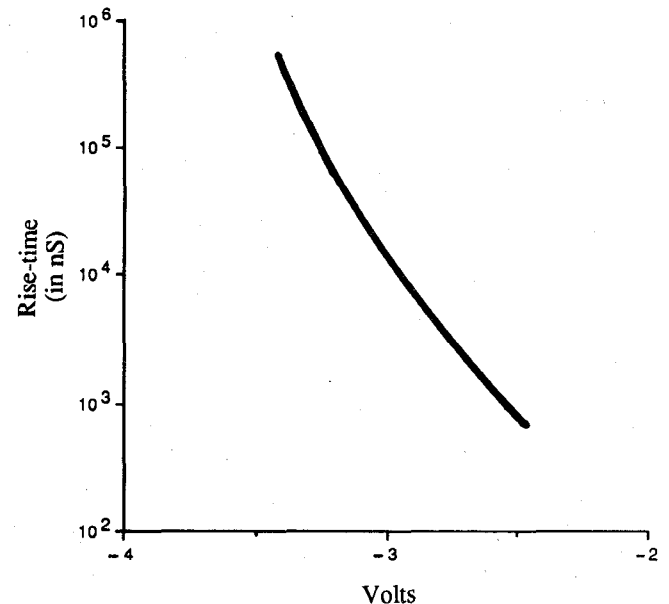
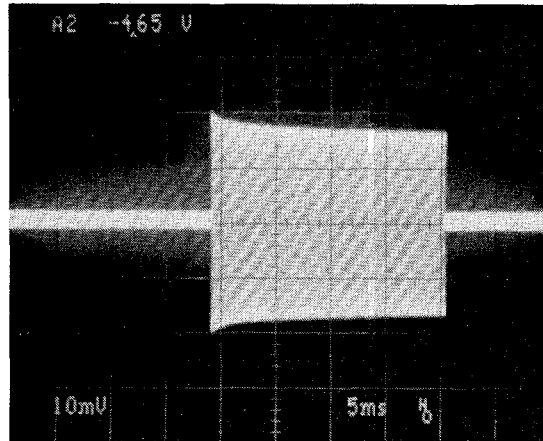


Fig. 7. Rise time for a variable attenuator as the MESFET control device is switched from -7 V to a variable voltage shown on the x axis.



Horizontal Scale 5 mS/div  
Vertical Scale 10 mV/div

Fig. 8. The overshoot of the RF signal for a FET with pinch-off voltage of -4.5 V as the gate voltage is switched from -4.95 to -4.05 V.

creating a depletion layer which extends beyond the normal gate depletion layer. This effect can be represented by an equivalent  $RC$  network, where the  $R$  represents the effective surface resistance (which is separated from the bulk region by a surface depletion layer) and  $C$  represents the resultant depletion layer capacitance. When the device is switched "on" the charge stored in surface-to-bulk depletion layer capacitance discharges through the large surface resistance; thus the channel immediately adjacent to the gate fails to respond to the new control voltage. We believe that this is the most dominant mechanism in determining long-term switching transients in FET's and variable attenuators.

In the nonconducting state, the gate is biased beyond pinch-off, and the voltage in excess of the pinch-off voltage is

mostly supported in the S.I. substrate. Under steady state, the deep traps in the S.I. substrate are deprived of electrons and thus the S.I. substrate below the channel is more positive than at zero gate bias. When the voltage at the gate is switched so that the channel is at least partially open, the relative positive charge in the S.I. substrate tends to accumulate electrons in the channel region, which leads to an overshoot in the transmitted RF signal.

The RF signal overshoot is shown in Fig. 8. Note the bias voltages are chosen so that the effect of electron accumulation has noticeable effect at the output. The deep traps in the channel also affect the RF transient, though the exact nature of the transient is now dependent on the characteristic of the traps [8].

## V. DISCUSSION

The analysis of the switching mechanisms in control MESFET's reveals many important aspects of MESFET switches. The dominant intrinsic switching speed limiting factor for a single control FET is the gate resistance in series with the gate-to-channel capacitance. The gate capacitance can be reduced by reducing the gate length, which will also improve the RF characteristics of the device [1]. The gate resistance improves the small-signal characteristics (insertion loss and isolation) and increases the dynamic power handling capability of FET's at high frequencies by effectively floating the gate [1].

However, this can also be achieved using a diode-gate FET [5], [6] with a low gate bias resistance (about  $100\ \Omega$ ). Thus, by reducing the gate length and gate bias resistance the intrinsic switching speed can be increased substantially.

The intrinsic switching speed models indicate an effective way of measuring the channel doping of the FET without destroying the FET's because the capacitance  $C_i$  is doping dependent. The capacitance can be calculated from the intrinsic signal transients. This procedure of measuring the doping densities is straightforward, though its accuracy in providing the exact doping profile requires further investigation.

Finally, the material-related transients determine the limit of the switching capability of the control FET. For a 3–5 V pinch-off device, the surface states determine the rise time. Earlier work indicates that this effect can be minimized by reducing the gate to recess separation [4]. For a multibit attenuator, innovative circuit designs using fewer cascaded FET's can significantly improve switching speeds [9].

## VI. CONCLUSIONS

In this paper modeling results show that the MESFET control device is inherently capable of switching in shorter times than are currently achieved (1–5 ns). Improvement in the nanosecond range switching transients is possible by using the diode-gate MESFET in series with a reduced gate-bias resistance and reduced gate lengths. Microsecond-to-millisecond transients are caused by material imperfections, particularly surface states, for present control devices. The effect of the S.I. substrate appears important in control MESFET's only under restricted bias conditions, namely when switching from slightly in pinch-off to slightly above pinch-off.

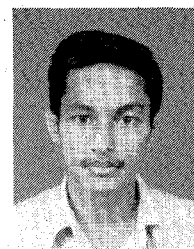
## ACKNOWLEDGMENT

The authors gratefully acknowledge the contributions of P. Ersland and J. Parker in establishing the measurement facilities and procedures. M. Heimlich and D. Hou for helpful technical discussions, and the GaAs MMIC control product group at M/A-COM ASD for processing and assembly.

## REFERENCES

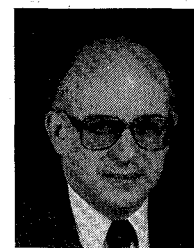
- [1] N. Jain, and R. J. Gutmann, "Broadband MESFET control device design," *IEEE Trans. Microwave Theory Tech.*, vol. 38, pp. 109–117, Feb. 1990.
- [2] S. Blight, R. H. Wallis, and H. Thomas, "Surface influence on the conductance DLTS spectra of GaAs MESFET's," *IEEE Trans. Electron Devices*, vol. ED-33, pp. 1447–1453, Oct. 1986.
- [3] M. Rocchi, "Status of the surface and bulk parasitic effects limiting the performance of GaAs IC's," *Physica*, vol. 129B, pp. 119–138, 1985.
- [4] R. Yeats *et al.*, "Gate slow transients in GaAs MESFETs—Cause, cures and impact on circuits," in *IEDM Tech. Dig.*, Dec. 1988, pp. 842–845.
- [5] N. Jain, R. J. Gutmann, D. Fryklund, and W. Moroney, "Low distortion GaAs MESFET control components for baseband applications," in *GaAs IC Symp. Dig.*, Oct. 1989, pp. 169–172.
- [6] N. Jain and R. J. Gutmann, "Improved GaAs MESFET switches for baseband applications," *Applied Microwave*, vol. 2, pp. 100–108, Summer 1990.
- [7] T. Takada, Y. Yokoyama, M. Ida, and T. Sudo, "A MESFET variable-capacitance model for GaAs integrated circuit simulation," *IEEE Trans. Microwave Theory Tech.*, vol. MTT-30, pp. 719–724, May 1982.
- [8] E. H. Rhoderick *Metal Semiconductor Contacts*. Oxford: Clarendon Press, 1978, ch. 4.
- [9] J. Bayruns, P. Wallace, and N. Scheinberg, "A monolithic dc–1.6 GHz digital attenuator," in *IEEE MTT-S Int. Microwave Symp. Dig.*, June 1989, pp. 1295–1298.

†



**Nitin Jain** received the B. Tech degree in electronic engineering from the Indian Institute of Technology, Madras, in 1986 and the M.S.E.E. degree in electrical engineering from Rensselaer Polytechnic Institute, Troy, NY, in 1989. He has worked for two summers at M/A-COM's Advanced Semiconductor Division on improved low-frequency power handling and switching characteristics of MESFET control components as part of his graduate program. At present, he is working towards the Ph.D. degree at Rensselaer and is supported by a M/A-COM fellowship. He is a recipient of an educational fellowship awarded by IEEE Microwave Theory and Techniques Society for 1990. His current research interests include microwave monolithic control devices and technology and related topics in solid-state physics.

†



**Ronald J. Gutmann** (S'58–M'63–SM'76) received the B.E.E. degree from Rensselaer Polytechnic Institute, Troy, NY, in 1962, the M.E.E. degree from New York University, New York, NY, in 1964, and the Ph.D. degree in electrophysics from Rensselaer Polytechnic Institute in 1970.

While an undergraduate, he was employed by the Microwave and Power Tube Division of Raytheon Company. From 1962 to 1966, he was a Member of the Technical Staff at

Bell Laboratories, where he worked on the development of microwave components and systems for radar applications. From 1966 to 1967, he was Senior Engineer at Lockheed Electronics Company, where he worked on beam-steering and beam-forming techniques for phased arrays. From 1967 to 1970, he was employed as a Research Assistant at Rensselaer Polytechnic Institute and as an Engineer at the Rensselaer Research Corporation, where he developed novel semiconductor control devices. Since 1970, Dr. Gutmann has been with Rensselaer Polytechnic Institute, where he is currently a Professor in the Electrical, Computer, and Systems Engineering Department with teaching and research activities in the areas of semiconductor devices, microwave techniques, radiation effects, nondestructive testing techniques, monolithic microwave integrated circuits, and interconnection technology. He has authored over one hundred technical papers in these and related fields.

Dr. Gutmann was a NASA-ASEE Fellow in 1977, performing microwave system studies at Johnson Space Center; a Visiting Member of the Technical Staff at Bell Laboratories in 1979, working on high frequency power converters; and a Visiting Scientist at M/A-COM in 1985, working on MESFET control devices. From May 1981 to August 1983 he served as Program Director of the Solid State and Microstructures Engineering Program at the National Science Foundation, where he chaired the Interagency Electronics Committee, served on the Technical Activities Board of the

SRC, and had administrative responsibility for the National Nanofabrication Facility. Since returning to Rensselaer, he has served as Chairman of the ECSE Executive Committee and Chair of the Rensselaer Faculty Council. He presently serves as Director of the Center for Integrated Electronics, an interdisciplinary research and education center with programs in electronic materials, processing techniques, semiconductor devices, characterization techniques, and VLSI design.

‡

**David M. Johnson** received the B.S.E.E. degree from the University of Lowell, Lowell, MA, in 1982.

From 1982 to 1989 he was employed as a design and development engineer for the GaAs FET product and control product groups at M/A-Com's Advanced Semiconductor Division. Presently he is employed at M/A-Com Anzac Division as a senior design and development engineer for the control product group. His present interests lie in the development of MMIC GaAs FET control products and their design into hybrid circuits.